Room Temperature Ionic Liquid in Confined Media: A Temperature Dependence Solvation Study in [bmim][BF4]/BHDC/Benzene Reverse Micelles

ARTICLE *in* THE JOURNAL OF PHYSICAL CHEMISTRY B · MAY 2011

Impact Factor: 3.3 · DOI: 10.1021/jp109088h · Source: PubMed

5 AUTHORS, INCLUDING:

Chiranjib Ghatak
University of Kansas
38 PUBLICATIONS **570** CITATIONS
SEE PROFILE

Vishal Govind Rao
Bowling Green State University
49 PUBLICATIONS **533** CITATIONS
SEE PROFILE

Nilmoni Sarkar
IIT Kharagpur
159 PUBLICATIONS **3,691** CITATIONS
SEE PROFILE

THE JOURNAL OF PHYSICAL CHEMISTRY B

ARTICLE

pubs.acs.org/JPCB

Room Temperature Ionic Liquid in Confined Media: A Temperature Dependence Solvation Study in [bmim][BF_4]/BHDC/Benzene Reverse Micelles

Rajib Pramanik, Chiranjib Ghatak, Vishal Govind Rao, Souravi Sarkar, and Nilmoni Sarkar*

Department of Chemistry, Indian Institute of Technology, Kharagpur 721302, WB, India

Supporting Information

ABSTRACT: In this work, we reported a detailed study of the solvation dynamics of coumarin-480 in [bmim][BF_4]/BHDC/benzene reverse micelles (RMs) with varying [bmim][BF_4]/BHDC molar ratio (R) 1.00, 1.25, 1.50, and also study the solvation dynamics at five different temperatures from 15 to 35 °C RMs at [bmim][BF_4]/BHDC molar ratio 1.25 for the first time. The average solvation time constant becomes slightly faster with the increase in R values at a temperature 25 °C. The solvation dynamics of the RMs with R value 1.25 becomes faster with the increase in temperature. We have also investigated temperature-dependent solvation dynamics in neat [bmim][BF_4]. The solvation dynamics in neat [bmim][BF_4] has a substantial temperature effect but for the [bmim][BF_4]/BHDC/benzene RMs the temperature effect on the solvation dynamics is not that significant. Time-resolved fluorescence anisotropy studies reveal a decrease in the rotational restriction on the probe with increasing temperature. Wobbling-in-cone analysis of the anisotropy data also supports this finding.

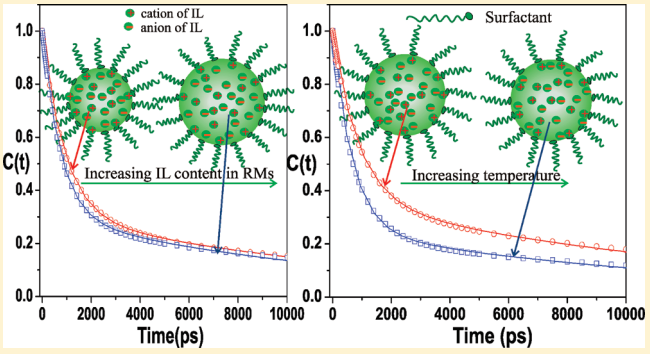

1. INTRODUCTION

Room temperature ionic liquids (RTILs) are believed to be environmentally friendly, nontoxic green solvents, having a melting point below room temperature, which is the reason why they have attracted a good deal of attention.[1] RTILs are organic salts composed entirely of ions, and unlike the common organic salts, which melt at high temperatures, these salts melt at low temperature primarily due to the fact that the constituent ions are fairly large with low charge density. Substituted imidazolium ions are the most popular cationic component of the RTILs and among the anions, $[BF_4]^-$, $[PF_6]^-$, and $[(CF_3SO_2)_2N]^-$ are most frequently used. Since the properties of RTILs are very much dependent on the constituent ions, it is possible to obtain an RTIL of a desired property by picking the right combination of the cationic and anionic constituents; these liquids are called "designer solvents".[2] The key feature of RTILs is its nonvolatile nature, so it can be used as an environmentally green solvent for the replacement of volatile organic compounds (VOCs) in organic synthesis. Besides this, most of the RTILs have some common feature such as a broad liquid temperature range (−96 to 300 °C), a high ion conductivity, wide electrochemical windows, and the ability to dissolve various organic or inorganic compounds to make them a green substitute for VOCs.[3−11] RTILs have been used as solvents in various chemical reactions[12−16] and in pharmaceutical synthesis.[17]

Studies on combinations of surfactants with ionic liquids have become an attractive topic.[18−20] The evidence of dry micelle formation of several traditional surfactants in IL media has appeared in the literature.[18] Han and co-workers[19] demonstrated that 1-butyl-3-methylimidazolium tetrafluoroborate ([bmim][BF_4]) could form polar nanosized droplets dispersed in a cyclohexane continuous phase, and Eastoe et al.[20] investigated the structure of the same system by small-angle neutron scattering (SANS), which showed a regular increase in droplet volume as micelles were progressively swollen with added [bmim][BF_4]. Following these discoveries of novel microemulsions, the formation mechanism of microemulsions containing an IL with the electropositive imidazolium ring was explored using spectroscopic techniques,[21] and some applications of these kinds of microemulsions in material preparation have also been attempted.[22] Falcone et al.[23] characterized novel reverse micelle (RM) systems consisting of two different ILs (1-butyl-3-methylimidazolium tetrafluoroborate ([bmim][BF_4]) and 1-butyl-3-methylimidazolium bis(trifluoromethylsulfonyl)imide ([bmim][Tf_2N])) sequestrated by two different surfactants (Triton X-100 (TX-100) and benzyl-n-hexadecyldimethylammonium chloride (BHDC)) in order to make IL/surfactant/benzene RMs.

In recent years, there has been a tremendous interest to investigate different types of physical and chemical properties of RTILs. Several physical, photophysical, and ultrafast

Received: September 23, 2010
Revised: March 30, 2011
Published: April 15, 2011

Scheme 1. Structures of C-480 and [bmim][BF_4]

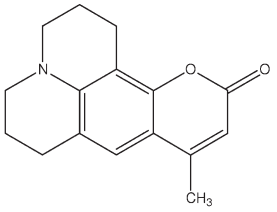

Coumarin-480

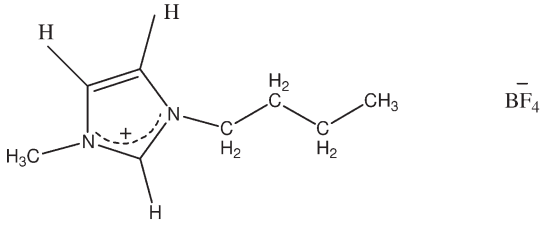

1-butyl-3-methyl imidazolium tetrafluoroborate (bmimBF_4)

spectroscopic studies have been carried out on these RTILs.[24−36] The nature of solvation in neat RTILs was investigated both experimentally and theoretically.[25−34] The solvation dynamics has also been studied in the mixtures of RTILs and conventional solvents[37,38] and in RTILs containing microheterogeneous systems.[39,40] Adhikari et al. investigated the dynamics in different regions of the 1-pentyl-3-methylimidazolium tetrafluoroborate ([pmim][BF_4]) containing microemulsions and also in neat [pmim][BF_4].[41] Previous studies carried out by our group showed the effect of confinement of the RTIL [bmim][BF_4] on solvent and rotational relaxation dynamics of C153 in [bmim][BF_4]/TX100/cyclohexane microemulsions.[42]

In the present study we investigated the effect of varying the [bmim][BF_4]/BHDC molar ratio (R) on the solvent relaxation of RTILs in [bmim][BF_4]/BHDC/benzene reverse micelles. We also attempted to study temperature-dependent solvation dynamics and rotational relaxation dynamics in neat [bmim][BF_4] and in [bmim][BF_4]/BHDC/benzene reverse micelles at a particular R value. To the best of our knowledge, no group has studied the solvation dynamics of RTILs containing reverse micelles as a function of temperature, whereas there are some reports on the effect of temperature on the solvation dynamics of an aqueous reverse micelle system.[43] It is known that ionic liquid microemulsion systems are very sensitive toward temperature.[44] The structure of these RMs at different temperatures was determined using a dynamic light scattering (DLS) technique. The structure of RTIL and coumarin-480 (C-480) are shown in Scheme 1.

2. EXPERIMENTAL SECTION

Coumarin-480 (C-480) (laser grade, Exciton) was used as received. 1-Butyl-3-methylimidazolium tetrafluoroborate ([bmim][BF_4]) was obtained from Kanto chemicals (99% purity). BHDC was purchased from Aldrich, and benzene was obtained from Spectrochem (UV spectroscopy grade). A stock solution of 0.4 M BHDC in benzene was prepared at room temperature (25 °C) by direct weighing. We used this 0.4 M solution for all the measurements. RTIL content of the RMs solution (R value) was expressed by the molar ratio of added RTIL to surfactant (BHDC), i.e. R = ([RTIL])/([BHDC]). We made the solution transparent by gently shaking by hand. Different sizes of RMs were prepared by varying the molar ratio (R) of [RTIL])/([BHDC]. The final concentration of C-480 in all experiments was kept at 10^{-5} (M).

The absorption and fluorescence spectra were measured using a Shimadzu (model no. UV-2450) spectrophotometer and a Hitachi F-7000 spectrofluorimeter. For steady-state experiments, all samples were excited at 408 nm. The detailed time-resolved fluorescence setup is described in our earlier publication.[25] Briefly, the samples were excited at 408 nm using a picosecond laser diode (IBH, Nanoled), and the signals were collected at a magic angle (54.7°) using a Hamamatsu microchannel plate photomultiplier tube (3809U). The instrument response function of our setup was 90 ps. The same setup was used for anisotropy measurements. For the anisotropy decays, we used a motorized polarizer in the emission side. The emission intensities at parallel ($I_{||}$) and perpendicular ($I_{\perp}$) polarizations were collected alternately until a certain peak difference between parallel ($I_{||}$) and perpendicular ($I_{\perp}$) decay was reached. The peak differences depended on the taild of the parallel ($I_{||}$) and perpendicular ($I_{\perp}$) decays matching. The analysis of the data was done using IBH DAS, version 6, decay analysis software. The same software was also used to analyze the anisotropy data. All the longer and shorter wavelength decays were fitted with biexponential and triexponential functions, respectively, because χ^2 becomes closer to 1, which indicates a good fit. For dynamic light scattering (DLS) measurements, we used a Malvern Nano ZS instrument employing a 4 mW He−Ne laser (λ = 632.8 nm). All the scattering photons were collected at a 173° scattering angle. The scattering intensity data were processed using the instrumental software to obtain the hydrodynamic diameter (d_h) and size distribution of each sample. The instrument measures the time-dependent fluctuation in the intensity of the light scattered from the particles in solution at a fixed scattering angle. The hydrodynamic diameter (d_h) of the reverse micelle was estimated from the intensity autocorrelation function of the time-dependent fluctuation in intensity. d_h is defined as

$$d_h = \frac{k_b T}{3\pi\eta D} \quad (1)$$

where k_b is the Boltzmann constant, η is the viscosity, and D is the translational diffusion coefficient. In a typical size distribution graph from the DLS measurement, the x-axis shows a distribution of size classes in nanometers, while the y-axis shows the relative intensity of the scattered light. For viscosity measurements we used a Brookfield DV-II+ Pro (Viscometer). Experiments were carried out at five different temperatures from 15 to 35 °C. The temperature was maintained as a constant by circulating water through the cell holder using a Lab. Companion Thermostat (RG-0525G).

3. RESULTS AND DISCUSSION

3.1. Steady-State Absorption and Emission Spectra. The absorption and emission spectra were taken in benzene and [bmim][BF_4]/BHDC/benzene reverse micelles. The absorption and emission maxima are listed in Supporting Information Table 1. The emission maxima of C-480 in benzene and [bmim][BF_4] ionic liquid are 423 and 462 nm respectively. On addition of

BHDC to a solution of C-480 in benzene, the emission maximum of C-480 exhibits a marked red shift from 423 to 448 nm. The marked red shift by 25 nm indicates transfer of the C-480 molecules from bulk benzene to the interior of BHDC reverse micelles. On addition of the RTIL ([bmim][BF_4]) to the BHDC/benzene mixture, the emission maximum of C-480 displays a further red shift by 9 to 457 nm (at λ_{ex} = 410 nm). The red shift suggests that a significant portion of the probe molecules is located inside the RMs. For the R = 1.25 systems, the emission maxima are obtained at 456 nm and remain unchanged upon an increase in temperature 15−35 °C which clearly signifies that the probe senses a similar environment at all the temperatures. It is observed that absorption and emission spectra of the probe C-480 in [bmim][BF_4] do not depend on the temperature. The absorbance at the red end of the spectrum increases with addition of [bmim][BF_4] to the C-480/BHDC/benzene solution. This indicates that a substantial number of C-480 molecules migrate from bulk solvent to the reverse micellar ionic liquid pool. The absorption and emission spectra of C-480 in RMs at different R values are illustrated in Supporting Information, Figure 1. The distribution of the solute between the surrounding solvent and the micelles can be described in terms of a partition constant. There are various methodologies that have been employed to obtain distribution constants of the probe molecules in two pseudophases.[45] To get the details of the probe location, we have carried out the partition coefficient study of C-480 in this RM system using the method applied by Novaira et al.[46] (for details, see the Supporting Information). It has been observed from Figure 4 (in the Supporting Information) that absorption and emission spectra of C-480 in the RMs (R = 1.25) at the temperature range from 15 to 35 °C are almost unaltered which certainly indicates that the partition of C480 between the two pseudophases (the organic and the micellar) does not change with variation of temperature.

It is known that certain dyes show thermochromism which is the reversible dependence of color on temperature, existing in a thermal equilibrium between two distinct and interconvertible isomeric species.[47] Thus, if thermochromism takes place in the case of C-480 dye in the present system, then absorption and emission spectra of the dye should have changed with change in temperature. We have studied absorption and emission spectra of C-480 dye dissolved in pure benzene and pure ionic liquids which are shown in Supporting Information Figures 5 and 6. It has been observed that there is no change in the absorption and emission spectra, which clearly indicates that thermochromism does not take place in C-480 dye.

3.2. Dynamic Light Scattering Study. Falcon et al.[23] reported that the droplet size increases when the [bmim][BF_4] content increases, which indicates that [bmim][BF_4] are sequestrated by the surfactants yielding [bmim][BF_4] RMs. The linear tendency observed at R values lower than 1.5 for the [bmim][BF_4] incorporated RM systems. They have explained the fact that, [bmim][BF_4] RM system shows a deviation from the linearity at R values higher than 1.5 due to droplet−droplet interaction is favored and changing the shape of the RMs. We have also observed the similar size variation with varying [bmim][BF_4] content in BHDC RMs. The hydrodynamics diameter (d_h) of the RMs of various R values as obtained from DLS measurements are shown in the Supporting Information Figure 7. The linear tendency observed at R values lower than 1.5 in the [bmim][BF_4] RM systems indicates that, under these conditions, the IL RMs are discrete and noninteracting spherical droplets. We have also measured the size of the RMs at varying temperature at specific R value. The inset of Figure 1 depicts the variation of the average hydrodynamic diameter at R = 1.25 of RMs as a function of temperature. It is evidenced from the dynamic light scattering study (shown in Figure 1) that, with the increase in temperature, the reverse micellar diameter changes marginally, and the measured hydrodynamic diameter is 19 nm (±1 nm).

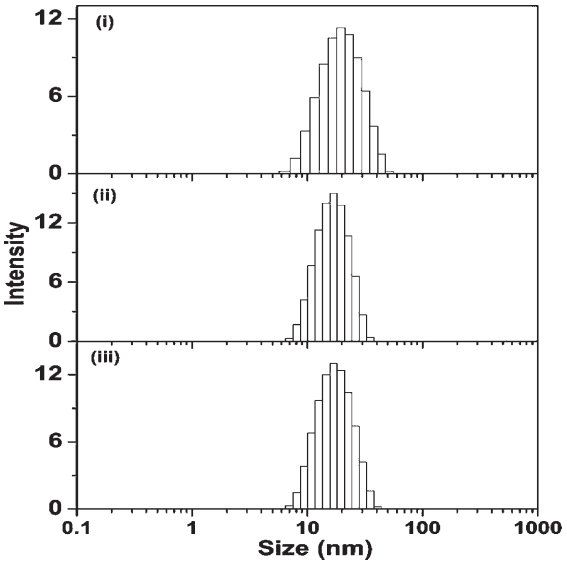

Figure 1. Size distribution of the droplets (measured by dynamic light scattering) in a RMs of [bmim][BF_4]/BHDC/benzene (R = 1.25) at (i) 15 °C, (ii) 25 °C and (iii) 35 °C respectively.

3.3. Viscosity Measurement. We have measured the viscosity of neat [bmim][BF_4] and [bmim][BF_4]/BHDC/benzene RMs at various temperature. With gradual increasing of temperature, the bulk viscosity of the neat [bmim][BF_4] and [bmim][BF_4]/BHDC/benzene RMs are gradually decreases. Strong electrostatic interaction between the anion and the imidazolium ring cation plays a major role for high viscosity in neat [bmim][BF_4]. With gradual increasing of temperature, electrostatic interaction between the anion and the imidazolium ring cation decreases as consequence viscosity decreases in neat [bmim][BF_4]. The viscosity of neat [bmim][BF_4] and [bmim][BF_4]/BHDC/benzene RMs at various temperature are listed in Table 1.

3.4. Time-Resolved Studies. *3.4.1. Time-Resolved Anisotropy Measurements.* Absorption and emission spectra can give a qualitative idea regarding the location of the probe molecules. This can be more accurately predicted by the time-resolved fluorescence anisotropy. Time resolved anisotropy, $r(t)$, is calculated using the following equation:[48]

$$r(t) = \frac{I_{\parallel}(t) - GI_{\perp}(t)}{I_{\parallel}(t) + 2GI_{\perp}(t)} \quad (2)$$

where G is the correction factor for detector sensitivity to the polarization direction of emission. $I_{\parallel}(t)$ and $I_{\perp}(t)$ are fluorescence decays, polarized parallel and perpendicular to the polarization of the excitation light, respectively. The G factor for our setup is 0.6. The anisotropy decay parameters are listed in Table 1. Representative anisotropy decays of C-480 in [bmim][BF_4]/BHDC/benzene (R = 1.25) reverse micelles at various temperatures are shown in Figure 2. The anisotropy decays in reverse micelles are found to be biexponential in nature.

Table 1. Anisotropy Decay Parameters of C480 in Neat [bmim][BF_4] and [bmim][BF_4] /BHDC/Benzene RMs at Different Temperatures

system	temp (°C)	a_1	a_2	τ_1 (ns)	τ_2 (ns)	$<\tau_{rot}>$ (ns)	viscosity (cP)	R_0
[bmim][BF_4]/BHDC/benzene RMs R = 1.25	15	0.62	0.38	0.21	1.34	0.64	3.2	0.32
	20	0.57	0.43	0.18	1.11	0.57	2.8	0.30
	25	0.61	0.39	0.18	1.07	0.53	2.5	0.28
	30	0.55	0.45	0.15	0.81	0.45	2.2	0.27
	35	0.54	0.46	0.13	0.65	0.37	2.0	0.28
[bmim][BF_4] + C-480	15		1		5.65	5.65	176	0.30
[bmim][BF_4] + C-480	20		1		4.73	4.73	135	0.31
[bmim][BF_4] + C-480	25		1		3.63	3.63	101	0.32
[bmim][BF_4] + C-480	30		1		3.00	3.00	81	0.32
[bmim][BF_4] + C-480	35		1		2.42	2.42	60.5	0.32

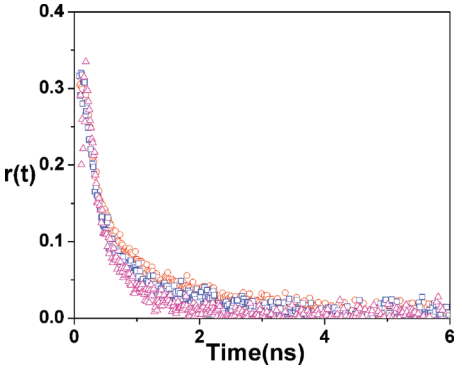

Figure 2. Fluorescence anisotropy decays of C-480 in [bmim][BF_4]/BHDC/benzene (R = 1.25) RMs at (i) 15 °C (red ○), (ii) 25 °C (blue □), and (iii) 35 °C (magenta △), respectively.

It can be observed from Table 1 that the time constant of both the faster and slower components decreases with increasing temperature. This certainly indicates that the probe is free to move at elevated temperatures. To understand the effect of temperature on the rotational relaxation process of the probe inside the reverse micelles in a more quantitative manner, the biexponential anisotropy decay was analyzed using the two-step and wobbling-in-cone models.[49−52] The two-step model shows that observed slow rotational relaxation (τ_2) is a convolution of the relaxation time corresponding to the overall rotation motion of the micelles (τ_m) and lateral diffusion of the probe (τ_D). The wobbling-in-cone model describes the internal motion of the probe (τ_e) in terms of a cone angle (θ_0) and wobbling diffusion coefficient (D_w). The τ_m, τ_D, τ_e, θ_0, and D_w values are calculated from the relevant equations defined by Quitevis et al.[53] as follows

$$\frac{1}{\tau_2} + \frac{1}{\tau_D} + \frac{1}{\tau_m} \tag{3}$$

$$\frac{1}{\tau_1} + \frac{1}{\tau_e} + \frac{1}{\tau_2} \tag{4}$$

where τ_1 and τ_2 are the observed fast and slow components, respectively. The results are summarized in Supporting Information, Table 2. Overall rotation of the reverse micelles can be estimated using the Stokes−Einstein−Debye relation.[53,54]

$$\tau_m = \frac{4\pi\eta r_h^3}{3kT} \tag{5}$$

where η is the viscosity of the benzene, r_h is the hydrodynamic radius of the RMs, and k and T are Boltzmann's constant and the absolute temperature, respectively. The calculated τ_m values are in the range of a several nanoseconds. It could be noted that the τ_m values are an order of magnitude higher than the τ_1 and τ_2 values. Therefore, overall rotation does not contribute to the anisotropy decays. This is because the reorientation time for the overall rotation of the reverse micelles becomes very long, and consequently the fluorescence depolarization due to this process becomes negligible. We have also calculated the order parameter (S) to get a clear idea about the location of the probe. The value of S is obtained from the relative amplitude of the slow component as

$$S^2 = a_2 \tag{6}$$

The magnitude of the S is a measure of spatial restriction and has values from zero (unrestricted motion) to 1 (completely restricted motions). The high value of the order parameter indicates that probe molecules are experiencing restricted motions, which is possible if they are located in the interface or core of the RMs. We can calculate the cone angle θ_0 and wobbling diffusion coefficient as follows.

$$\theta_0 = \cos^{-1}\left[\frac{1}{2}\{(1+8S)^{1/2} - 1\}\right] \tag{7}$$

$$D_w + \frac{7\theta^2}{24\tau_e} \tag{8}$$

where θ_0 is cone angle in radians. The D_w value of C-480 increases with an increasing the temperature. This indicates that the microviscosity experienced by the probe decreases with an increase in temperature. With an increase in temperature, C-480 molecules experience less friction due to increased internal motions of ions of [bmim][BF_4] in the RMs; thus, microviscosity also decreases, and the value of D_w increases.

We also studied the rotational relaxation time of C-480 in neat [bmim][BF_4] with change in temperature 288−308 K at three different temperatures (Figure 3). Anisotropy decays were single exponential at all temperatures. With an increase in temperature from 15 to 35 °C, the average rotational relaxation time gradually decreases from 5.65 to 2.42 ns (Table 1). The rotational times of C-480 in the [bmim][BF_4]/BHDC/benzene RMs (R = 1.25) are 0.64 and 0.37 ns at temperatures 288 K and 308 K, respectively. The rotational relaxation time of C-480 in [bmim][BF_4]/

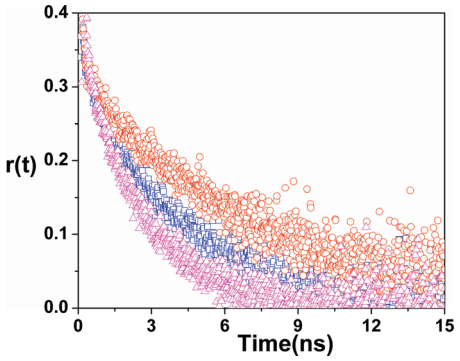

Figure 3. Fluorescence anisotropy decays of C-480 in neat [bmim][BF_4] at (i) 15 °C (red ○), (ii) 25 °C (blue □), and (iii) 35 °C (magenta △), respectively.

BHDC/benzene RMs is much less compared to that in neat [bmim][BF_4] at all the temperatures. Thus, the frictions of RTILs in RMs are very much different from that in neat RTILs.

3.4.2. Solvation Dynamics. To study solvent relaxation dynamics we collected the time-resolved decays monitored at different wavelength for all the systems. The decays at the red edge of the emission spectra were preceded by a growth in fraction of nanosecond time scale, while decays at the short wavelengths are fast. The wavelength-dependent behavior of temporal decays of C-480 clearly indicates that solvent relaxation is taking place in these systems. The time-resolved emission spectra (TRES) were constructed using the procedure of Fleming and Maroncelli.[55] The TRES at a given time t, $S(\lambda; t)$, is obtained by the fitted decays, $D(t; \lambda)$, by relative normalization to the steady-state spectrum $S_0(\lambda)$, as follows.

$$S(\lambda;t) = D(\lambda;t)\frac{S_0(\lambda)}{\int_0^\infty D(\lambda;t)\mathrm{d}t} \tag{9}$$

Each TRES was fitted by a log-normal line shape function, which is defined as

$$g(\nu) = g_0 \exp\left[-\ln 2\left(\frac{\ln[1+2b(\nu-\nu_p)]/\Delta}{b}\right)^2\right] \tag{10}$$

where g_0, b, ν_p, and Δ are the peak height, asymmetric parameter, peak frequency, and width parameter, respectively. We have obtained the peak frequency from the log-normal fitting of TRES. The solvation dynamics was monitored by the solvent response function defined as

$$C(t) = \frac{\nu(t)-\nu(\infty)}{\nu(0)-\nu(\infty)} \tag{11}$$

where $\nu(0)$, $\nu(t)$, and $\nu(\infty)$ are the peak frequencies at time 0, t, and infinity, respectively. In order to get $\upsilon(t = 0)$ value we have extrapolated $\upsilon(t)$ data to $t \rightarrow 0$ because of the limited time resolution of the instrument (90 ps). The solvent response function ($C(t)$) was fitted to a biexponential decay function

$$C(t) = a_1\, e^{(-t/\tau_1)} + a_2\, e^{(-t/\tau_2)} \tag{12}$$

where τ_1 and τ_2 are the two relaxation times with amplitudes a_1 and a_2, respectively.

First, we are going to discuss the important features of solvation dynamics in pure room-temperature ionic liquids. In a polar solvent such as methanol, water, or acetonitrile, the solvation process is extremely rapid. In molecular solvents, the reorientation of the solvent molecules around the photoexcited molecule is responsible for solvation, whereas in neat RTILs, the diffusional motion of the constituent cations and anions contributes to the solvation. The solvation time in most conventional solvents falls in the range 0.1−10 ps,[56] whereas the solvation time in neat RTILs is much larger, falling in the range 0.1−10 ns. Chapman and Maroncelli[57] showed that ionic solvation is slower compared to that in the pure solvent and is dependent on the viscosity of the medium. Bart et al.[58] showed that ionic solvation is slow and biphasic in nature. Since the motions of ions are responsible for solvation in RTILs, we observed biphasic dynamics in [bmim][BF_4] as compared to the monophasic dynamics observed in some conventional solvent molecules. Samanta et al.[59] reasoned that the fast component is due to the anions and the slow component is attributed to large-scale rearrangement of the ions around the photoexcited system. Petrich and co-workers observed that the polarizability of the cation is responsible for the fast component.[60] While Shim et al.[61] have shown that the short component is due to the translational motion of the anion, Kobrak and Znamenskiy, on the other hand, have demonstrated that collective cation−anion motion is responsible for the fast component.[62] Kashyap and Biswas[63] noted the dipolar nature of the imidazolium cations and thought that the dipole−dipole interactions might play an important role in the solvent stabilization of the fluorescent state of the dipolar molecules and, hence, can contribute to the dynamic Stokes shift. Their recent study showed that dipole−ion interaction contribution to the shift displays stronger temperature dependence than the dipole−dipole interaction component.[64]

In neat [bmim][BF_4], the average solvation time of C-480 at 288 K is 0.99 ns with components 0.37 ns (59%) and 1.88 ns (41%). At the elevated temperature of 308 K, the average solvation time of C-480 is 0.41 ns with components 0.18 ns (61%) and 0.76 ns (39%) (Table 2). Thus, with increasing temperature from 15 to 35 °C the average solvation time of C-480 in neat [bmim][BF_4] decreases 59%. With an increase in temperature 15 to 35 °C, the bulk viscosity of neat [bmim][BF_4] decreases from 176 cP to 60 cP (Table 1) because electrostatic interaction between the anion and cation are weakened at elevated temperature which reduces viscosity. Since at elevated temperature the electrostatic interaction is weaker, the diffusional motions of ions of [bmim][BF_4] increase, leading to faster solvation dynamics occuring at higher temperature (Figure 4).

From partition coefficient measurement of the probe it has been observed that a very small fraction of probe molecules stay in the bulk nonpolar solvent of [bmim][BF_4]/ BHDC/benzene RMs. However, these probes do not exhibit solvation dynamics in bulk nonpolar solvent. Therefore, we may neglect their contribution to the observed solvation dynamics. Furthermore, we have excited the probe molecules at the red end of the absorption spectra of C-480 (λ_{exc} = 408 nm) where probe molecules are selectively excited at the more polar region. In [bmim][BF_4]/BHDC/benzene RMs we have observed a bimodal solvation time in all the R values. The solvent relaxation in RTILs depends on translational motions of ions of the RTILs. There are two types of RTILs present in RMs that are in different environments, near and apart from headgroups of surfactants. The RTILs present near the surfactant molecule, that is at the interfacial regions, are more restricted due to translational

dx.doi.org/10.1021/jp109088h |*J. Phys. Chem. B* 2011, 115, 5971–5979

Table 2. Decay Parameters of $C(t)$ of C480 in Neat [bmim][BF_4] and [bmim][BF_4]/ BHDC/Benzene RMs at Different Temperatures

system	temp. (° C)	a_1	a_2	τ_1 (ns)	τ_2 (ns)	$<\tau_{avs}>$ (ns)	size (nm)
[bmim][BF_4]/BHDC/Benzene RMs R = 1.25	15	0.63	0.37	0.90	14.33	5.87	20
	20	0.69	0.31	0.87	14.15	4.98	19
	25	0.69	0.31	0.82	13.13	4.63	18
	30	0.70	0.30	0.72	12.08	4.12	18
	35	0.75	0.25	0.68	12.08	3.53	18
R = 1.00	25	0.69	0.31	0.92	13.72	4.89	12
R = 1.50	25	0.70	0.30	0.75	12.49	4.27	24
[bmim][BF_4] + C-480	15	0.59	0.41	0.37	1.88	0.99	
[bmim][BF_4] + C-480	20	0.65	0.35	0.34	1.62	0.79	
[bmim][BF_4] + C-480	25	0.58	0.42	0.22	1.15	0.61	
[bmim][BF_4] + C-480	30	0.60	0.40	0.21	0.90	0.49	
[bmim][BF_4] + C-480	35	0.61	0.39	0.18	0.76	0.41	

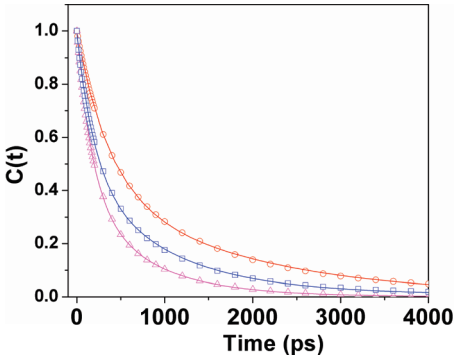

Figure 4. Decays of the solvent response functions, $C(t)$ of C-480 in neat [bmim][BF_4] at (i) 15 °C (red ○), (ii) 25 °C (blue □), and (iii) 35 °C (magenta △), respectively.

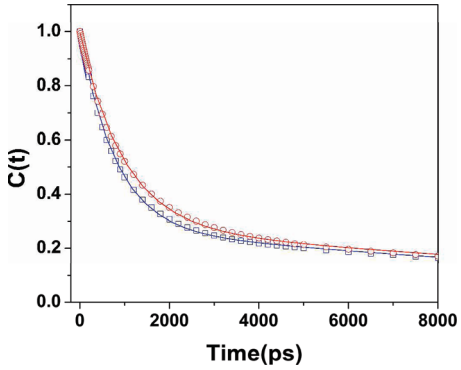

Figure 5. Decays of the solvent response functions, $C(t)$ of C-480 in [bmim][BF_4]/BHDC/benzene RMs at (i) R = 1.00 (red ○), and (ii) R = 1.50 (blue □) respectively.

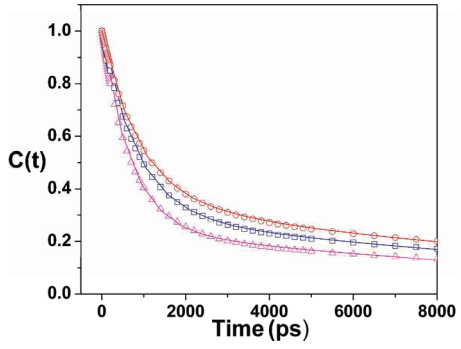

Figure 6. Decays of the solvent response functions, $C(t)$ of C-480 in [bmim][BF_4]/BHDC/benzene (R = 1.25) RMs at (i) 15 °C (red ○), (ii) 25 °C (blue □), and (iii) 35 °C (magenta △), respectively.

motions of the ions compared to the RTILs apart from surfactants molecules in RMs. So the slow components are arising due to RTIL molecules present at the interfacial regions of the RMs. The RTIL molecules being apart from surfactant molecules contribute to the fast component of solvation dynamics. In the RMs at R = 1.0, the average solvation time is 4.89 ns with time constants 0.92 ns (69%) and 13.72 ns (31%). At R = 1.25 (4.63 ns), the solvation time is very close to the value at R = 1.0. Upon further addition of [bmim][BF_4] the average solvation time decreases in very small magnitude, and at R= 1.50, it becomes 4.27 ns with time constants 0.75 ns (70%) and 12.49 ns (30%), respectively (Table 2). The size of the [bmim][BF_4]/BHDC/benzene RMs at R = 1.0 is 12 nm, and it has been observed that there is an increase in the droplet size when the [bmim][BF_4] content increases: the observed size of the RMs are 18 and 24 nm at R = 1.25 and R = 1.5, respectively (Table 2). The solvation relaxation of [bmim][BF_4] in RMs is almost independent of the [bmim][BF_4] content or the size of the RMs (Figure 5). The R independency of solvation time in [bmim][BF_4]/BHDC/benzene RMs is not similar to that in the hydrogen-bonded solvents, e.g. water,[65] methanol,[66] and glycerol[67] containing reverse micelles; that is, solvation time decreases with increasing w values in all the cases but is similar to that in non-hydrogen-bonded solvents such as acetonitrile[66] because solvation time is not affected by the change in the ratio, w. Shirota et al.[68] have observed that the solvation dynamics of aprotic dimethylformamide (DMF) in reverse micelles showed a tiny w dependence of the reverse micelle solution in contrast to protic formamide (FA) in reverse micelles that depends strongly on the w on the solvation dynamics.

Here, we have also studied the solvation dynamics of the probe in [bmim][BF_4]/BHDC/benzene RMs at different temperature. Temperature-dependent $C(t)$ plots in [bmim][BF_4] /BHDC/benzene RMs are shown in Figure 6. The solvation obtained in

dx.doi.org/10.1021/jp109088h |J. Phys. Chem. B 2011, 115, 5971–5979

the present study is broadly due to the ionic liquid present in different locations in the RMs. In this regard, one could average out the slow and fast components, which in turn are both slower as compared to the neat ionic liquid solvation. It is evidenced from Table 2 that one component is of the order of several hundreds of picoseconds, while the other is of the order of several nanoseconds. The observed slow time scales (on the order of a few nanoseconds) of the present system are due to the slow-moving interfacial ionic liquids. The contribution of the ionic liquid becomes decreased with an increase in temperature, and the fast components are originating due to the motions of ionic liquid present in the reverse micellar core. The contribution becomes increased with an increase in temperature. The overall decrease of solvation time on increasing temperature for $R = 1.25$ systems indicates that an increase in temperature accelerates the solvation process at the interface irrespective of the ionic liquid pool size. It is inferred from Table 2 that the solvation dynamics in neat [bmim][BF_4] is affected substantially by the temperature; however, for the [bmim][BF_4]/BHDC/benzene RMs the temperature effect on the solvation dynamics is not that significant. This is because the effect of motions of the ions of RTILs in (RMs) upon varying temperatures is less susceptible compared than that of bulk RTIL.

In the present RMs systems we have miss a considerable fraction of Stokes shift due to our limited instrumental resolutions, and we determined the loss in the dynamic Stokes shift using the procedure developed by Fee and Maroncelli,[69] where $\nu(0)$ can be calculated by the following equation:

$$\nu^{p}_{em}(0) = \nu^{p}_{abs} - [\nu^{np}_{abs} - \nu^{np}_{em}] \quad (13)$$

where ν^{p}_{abs}, ν^{np}_{abs}, and ν^{np}_{em} are the absorption peaks in polar solvent, absorption peak in nonpolar solvent, and emission peak in nonpolar solvent, respectively. We calculated the loss of dynamical Stokes shift in RMs at 298 K for $R = 1.0$, $R = 1.25$, $R = 1.5$ are 30%, 33%, and 34%, respectively. We also calculated loss of dynamical Stokes shift at $R = 1.25$ values at various temperatures; the loss is 30% at 288 K and 37% at 308 K. This is accompanied by decrease in the average solvation time ($<\tau_{solv}>$) from 5.87 to 3.53 ns by increasing temperature from 15 to 35 °C in RMs (Table 2). The decrease in dynamic stokes shifts and average solvation time with increase in temperature implies that the solvation dynamics is faster in the RMs.

4. ACTIVATION ENERGY

The temperature-dependent average solvation time and rotational time are used to calculate the activation energies (E_a) related with the solvation and rotational relaxation processes in the neat RTIL and in RMs. Figure 7 displays the Arrhenius plot of C480 in neat [bmim][BF_4] and RMs in the temperature range of 15−35 °C. Assuming Arrhenius dependence of the rate constant ($1/\tau$), the activation energy (E_a) has been evaluated from the logarithmic plot of $1/\tau$ against $1/T$. The E_a obtained from the average solvation times for [bmim][BF_4] and in RMs are 33.65 and 18.28 kJ/mol, respectively. Recently, Biswas et al.[64] experimentally measured activation energy (E_a = 33.1) for [bmim][BF_4] which is almost the same as our measured value. Further, the E_a's obtained for [bmim][BF_4] and [bmim][BF_4] in RMs from the calculated average rotational relaxation times are 32.49 and 20.11 kJ/mol, respectively. We obtained a large E_a

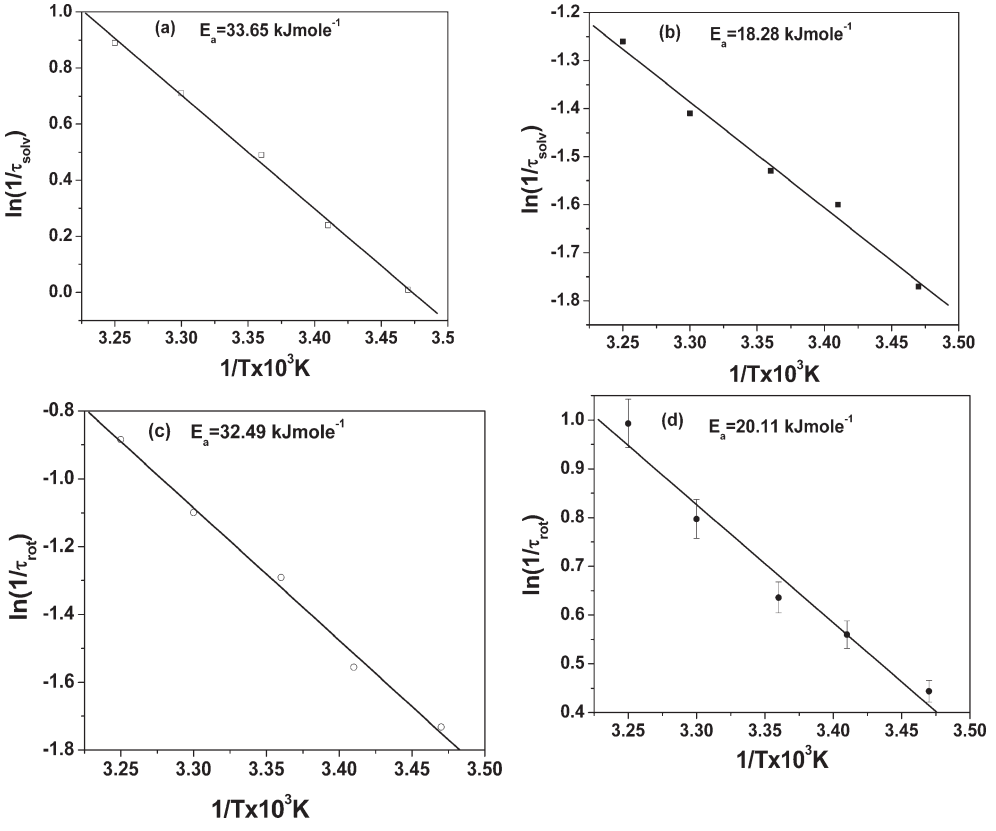

Figure 7. Plot of $\ln(1/\tau_{solv})$ against $1/T$ in (a) neat [bmim][BF_4] and in (c) [bmim][BF_4]/ BHDC/benzene RMs. Plot of $\ln(1/\tau_{rot})$ against $1/T$ in (b) neat [bmim][BF_4] and in (d) [bmim][BF_4]/BHDC/benzene RMs.

dx.doi.org/10.1021/jp109088h |J. Phys. Chem. B 2011, 115, 5971–5979

value in neat [bmim][BF_4] compared to that in RTIL containing RMs. The large values of E_a clearly indicate stronger dependence of solvation and rotational relaxation on temperature in [bmim][BF_4] than that for RMs. Since diffusional motion of constituent ions of RTILs is responsible for solvation in RTILs, we can say from activation energy values that the change in diffusional motions of ions of RTILs in confined media (RMs) with varying temperature is less compared to that of diffusional motion of bulk RTIL.

5. CONCLUSIONS

Our studies explored the dynamics of solvent relaxation of a probe, C-480, at the polar interfacial region of [bmim][BF_4]/BHDC/benzene RMs with various R values which showed a tiny R dependence. We have also studied the temperature-dependent solvation dynamics of neat ionic liquid and ionic liquid RMs. The overall decrease of solvation time on increasing temperature for R = 1.25 systems indicates that an increase in temperature accelerates the solvation process at the interface, irrespective of the ionic liquid pool size. The solvation dynamics in neat [bmim][BF_4] has a substantial temperature effect, whereas for the [bmim][BF_4]/BHDC/benzene RMs the temperature effect on the solvation dynamics is not that significant.

■ ASSOCIATED CONTENT

Supporting Information. Representative absorption, emission spectra, and procedure for partition coefficient measurements. This material is available free of charge via the Internet at http://pubs.acs.org.

■ AUTHOR INFORMATION

Corresponding Author

*E-mail: nilmoni@chem.iitkgp.ernet.in. Fax: 91-3222-255303.

■ ACKNOWLEDGMENT

N.S. is grateful to the Council of Scientific and Industrial Research (CSIR) and the Board of Research in Nuclear Sciences (BRNS) Government of India for generous research grants. R.P., C.G., and V.G.R are grateful to the CSIR for research fellowships. S.S is grateful to the BRNS for SRF.

■ REFERENCES

(1) Welton, T. *Chem. Rev.* **1999**, *99*, 2071.
(2) Rogers, R. D.; Seddon, K. R. *Science (Washington, DC, U.S.)* **2003**, *302*, 792.
(3) Parvulescu, V. I.; Hardacre, C. *Chem. Rev.* **2007**, *107*, 2615.
(4) Chowdhury, S.; Mohan, R. S.; Scott, J. L. *Tetrahedron* **2007**, *63*, 2363.
(5) Wasserscheid, P.; Keim, W. *Angew. Chem., Int. Ed.* **2000**, *39*, 3772.
(6) Seddon, K. R. *Nat. Mater.* **2003**, *2*, 363.
(7) Plechkova, N. V.; Seddon, K. R. *Chem. Soc. Rev.* **2008**, *37*, 123.
(8) Welton, T. *Coord. Chem. Rev.* **2004**, *248*, 2459.
(9) Hagiwara, R.; Ito, Y. *J. Fluorine Chem.* **2000**, *105*, 221.
(10) Dupont, J.; de Souza, R. F.; Suarez, P. A. Z. *Chem. Rev.* **2002**, *102*, 3667.
(11) Sheldon, R. *Chem. Commun. (Cambridge, U.K.)* **2001**, 2399.
(12) Earle, M. J.; McCormac, P. B.; Seddon, K. R. *Green Chem.* **1999**, *1*, 23.
(13) Lee, C. W. *Tetrahedron Lett.* **1999**, *40*, 2461.
(14) Earle, M. J.; Seddon, K. R.; Adams, C. J.; Roberts, G. *Chem. Commun. (Cambridge, U.K.)* **1998**, 2097.
(15) Surette, J. K. D.; Green, L.; Singer, R. D. *Chem. Commun. (Cambridge, U.K.)* **1996**, 2753.
(16) Carmichael, A. J.; Haddleton, D. M.; Stefan, A. F. B.; Seddon, K. R. *Chem. Commun. (Cambridge, U.K.)* **2000**, 1237.
(17) Earle, M. J.; Seddon, K. R.; McCormac, P. B. *Green Chem.* **2000**, *2*, 261.
(18) (a) Merrigan, T. L.; Bates, E. D.; Dorman, S. C.; Davis, J. H. *Chem. Commun.* **2000**, 2051. (b) Anderson, J. L.; Pino, V.; Hagberg, E. C.; Sheares, V. V.; Armstrong, D. W. *Chem. Commun.* **2003**, 2444. (c) Fletcher, K. A.; Pandey, S. *Langmuir* **2004**, *20*, 33. (d) Patrascu, C.; Gauffre, F.; Nallet, F.; Bordes, R.; Oberdisse, J.; de lauth-Viguerie, N.; Mingotaud, C. *Chem. Phys. Chem.* **2006**, *7*, 99. (e) Velasco, S. B.; Turmine, M.; Caprio, D. D.; Letellier, P. *Colloids Surf., A* **2006**, *275*, 50.
(19) Gao, H. X.; Li, J. C.; Han, B. X.; Chen, W. N.; Zhang, J. L.; Zhang, R.; Yan, D. D. *Phys. Chem. Chem. Phys.* **2004**, *6*, 2914.
(20) Eastoe, S.; Gold, S. E.; Rogers, A.; Paul, T.; Welton, R. K.; Heenan, I. G. *J. Am. Chem. Soc.* **2005**, *127*, 7302.
(21) Gao, Y. A.; Zhang, J.; Xu, H. Y.; Zhao, X. Y.; Zheng, L. Q.; Li, X. W.; Yu, L. *ChemPhysChem.* **2006**, *7*, 1554.
(22) Yan, F.; Texter, J. *Chem. Commun.* **2006**, 2696.
(23) Falcone, R. D.; Correa, N. M.; Silber, J. J. *Langmuir* **2009**, *25*, 10426.
(24) Sarkar, A.; Trivedi, S.; Pandey, S. *J. Phys. Chem. B* **2009**, *113*, 7606.
(25) Aki, S. N. V. K.; Brennecke, J. F.; Samanta, A. *Chem. Commun.* **2001**, 413.
(26) Muldoon, M. J.; Gordon, C. M.; Dunkin, I. R. *J. Chem. Soc., Perkin Trans.* **2001**, *2*, 33.
(27) Reichardt, C. *Green Chem.* **2005**, *7*, 339.
(28) (a) Saha, S.; Mandal, P. K.; Samanta, A. *Phys. Chem. Chem. Phys.* **2004**, *6*, 3106. (b) Paul, A.; Samanta, A. *J. Phys. Chem. B* **2007**, *111*, 4724.
(29) Ingram, J. A.; Moog, R. S.; Ito, N.; Biswas, R.; Maroncelli, M. *J. Phys. Chem. B* **2003**, *107*, 5926.
(30) Arzhantsev, S.; Jin, H.; Baker, G. A.; Maroncelli, M. *J. Phys. Chem. B* **2007**, *111*, 4978.
(31) Mukherjee, P.; Crank, J. A.; Sharma, P. S.; Wijeratne, A. B.; Adhikary, R.; Bose, S.; Armstrong, D. W.; Petrich, J. W. *J. Chem. Phys. B* **2008**, *112*, 3390.
(32) Baker, S. N.; Baker, G. A.; Munson, C. A.; Chen, F.; Bukowski, E. J.; Cartwright, A. N.; Bright, F. V. *Ind. Eng. Chem. Res.* **2003**, *42*, 6457.
(33) (a) Kobark, M. N. *J. Chem. Phys.* **2006**, *125*, 064502. (b) Shim, Y.; Kim, H. J. *ACS Nano* **2009**, *3*, 1693.
(34) (a) Hu, Z.; Margulis, C. J. *Acc. Chem. Res.* **2007**, *40*, 1097. (b) Shim, Y.; Jeong, D.; Manjari, S.; Choi, M. Y.; Kim, H. J. *Acc. Chem. Res.* **2007**, *40*, 1130. (c) Castner, E. W., Jr.; Wishart, J. F.; Shirota, H. *Acc. Chem. Res.* **2007**, *40*, 1217.
(35) Chakrabarty, D.; Chakraborty, A.; Seth, D.; Sarkar, N. *J. Phys. Chem. A* **2005**, *109*, 1764.
(36) Shirota, H.; Funston, A. M.; Wishart, J. F.; Castner, E. W., Jr. *J. Chem. Phys.* **2005**, *122*, 184512.
(37) Pramanik, R.; Rao, V. G.; Sarkar, S.; Ghatak, C.; Setua, P.; Sarkar, N. *J. Phys. Chem. B* **2009**, *113*, 8626.
(38) Paul, A.; Samanta, A. *J. Phys. Chem. B* **2008**, *112*, 947.
(39) Chakraborty, A.; Seth, D.; Chakrabarty, D.; Setua, P.; Sarkar, N. *J. Phys. Chem. A* **2005**, *109*, 11110.
(40) Sasmal, D. K.; Mojumdar, S. S.; Adhikari, A.; Bhattacharyya, K. *J. Phys. Chem. B* **2010**, *114*, 4565.
(41) Adhikari, A.; Sahu, K.; Dey, S.; Ghosh, S.; Mandal, U.; Bhattacharyya, K. *J. Phys. Chem. B* **2007**, *111*, 12809.
(42) Chakrabarty, D.; Seth, D.; Chakraborty, A.; Sarkar, N. *J. Phys. Chem. B* **2005**, *109*, 5753.
(43) Mitra, R. K.; Sinha, S. S.; Pal, S. K. *Langmuir* **2008**, *24*, 49.
(44) Gao, Y.; Li, N.; Hilfert, L.; Zhang, S.; Zheng, L; Yu, L. *Langmuir* **2009**, *25*, 1360.
(45) Silber, J. J.; Biasutti, A.; Abuinb, E.; Lissib, E. *Adv. Colloid Interface Sci.* **1999**, *82*, 189.

(46) Novaira, M.; Biasutti, M. A.; Silber, J. J.; Correa, N. M. *J. Phys. Chem. B* **2007**, *111*, 748.
(47) (a) Tajima, M.; Inoue, H.; Hida, M. *Dyes Pigm.* **1987**, *8*, 119. (b) Tajima, M.; Sugai, M.; Matsunaga, K.; Yamashita, T.; Inoue, H.; Hida, M. *Dyes Pigm.* **1998**, *39*, 97.
(48) (a) Lakowicz, J. R. *Principles of Fluorescence Spectroscopy*, 2nd ed.; Kluwer, Plenum: Dordrecht, NY, 1999. (b) Birks, J. B. *Photophysics of Aromatic Molecules*; Wiley-Interscience: New York, 1970. (c) Turro, N. J. *Modern Molecular Photochemistry*; University Science Books: Sausalito, CA, 1991. (d) Gore, M. G. *Spectrophotometry and Spectrofluorimetry*; Oxford University Press: London, 2000. (e) Rettig, W.; Strehmel, B.; Schrader, S.; Seifert, H. *Applied Fluorescence in Chemistry, Biology, and Medicine*; Springer: New York, 1999. (f) Guilbault, G. G. *Practical Fluorescence*; Dekker: New York, 1990.
(49) Lipari, G.; Szabo, A. *J. Chem. Phys.* **1981**, *75*, 2971.
(50) Lipari, G.; Szabo, A. *J. Am. Chem. Soc.* **1982**, *104*, 4546.
(51) Lipari, G.; Szabo, A. *Biophys. J.* **1980**, *30*, 489.
(52) Wang, C. C.; Pecora, R. *J. Chem. Phys.* **1980**, *72*, 5333.
(53) Quitevis, E. L.; Marcus, A. H.; Fayer, M. D. *J. Phys. Chem.* **1993**, *97*, 5762.
(54) Maiti, N. C.; Krishna, M. M. G; Britto, P. J.; Periasamy, N. *J. Phys. Chem. B* **1997**, *101*, 11051.
(55) Maroncelli, M.; Fleming, G. R. *J. Chem. Phys.* **1987**, *86*, 6221.
(56) (a) Rosenthal, S. J.; Xie, X.; Du, M.; Fleming, G. R. *J. Chem. Phys.* **1991**, *95*, 4715. (b) Maroncelli, M. *J. Chem. Phys.* **1991**, *94*, 2084. (c) Jimenez, R.; Fleming, G. R.; Kumar, P. V.; Maroncelli, M. *Nature* **1994**, *369*, 471. (d) Castner, E.; Maroncelli, M.; Fleming, G. R. *J. Chem. Phys.* **1987**, *86*, 1090. (e) Rosenthal, S. J.; Jimenez, R.; Fleming, G. R.; Kuman, P. V.; Maroncelli, M. J. *Mol. Liq.* **1994**, *60*, 25.
(57) Chapman, C. F.; Maroncelli, M. *J. Phys. Chem.* **1991**, *95*, 9095.
(58) (a) Bart, E.; Meltsin, A.; Huppert, D. *J. Phys. Chem.* **1994**, *98*, 10819. (b) Bart, E.; Meltsin, A.; Huppert, D. *J. Phys. Chem.* **1994**, *98*, 3295.
(59) (a) Karmakar, R.; Samanta, A. *J. Phys. Chem. A* **2002**, *106*, 4447. (b) Karmakar, R.; Samanta, A. *J. Phys. Chem. A* **2002**, *106*, 6670. (c) Samanta, A. *J. Phys. Chem. Lett.* **2010**, *1*, 1557.
(60) Chowdhury, P. K.; Halder, M.; Sanders, L.; Calhoun, T.; Anderson, J. L.; Armstrong, D. W.; Song, X.; Petrich, J. W. *J. Phys. Chem. B* **2004**, *108*, 10245.
(61) (a) Shim, Y.; Duan, J. S.; Choi, M. Y.; Kim, H. J. *J. Chem. Phys.* **2003**, *119*, 6411. (b) Shim, Y.; Choi, M. Y.; Kim, H. J. *J. Chem. Phys.* **2005**, *122*, 44511.
(62) Kobrak, M. N.; Znamenskiy, V. *Chem. Phys. Lett.* **2004**, *395*, 127.
(63) (a) Kashyap, H. K.; Biswas, R. *J. Phys. Chem. B* **2008**, *112*, 12431. (b) Kashyap, H. K.; Biswas, R. *J. Phys. Chem. B* **2010**, *114*, 254.
(64) Kashyap, H. K.; Biswas, R. *J. Phys. Chem. B* **2010**, *114*, 16811.
(65) Sarkar, N.; Das, K.; Datta, A.; Das, S.; Bhattacharyya, K. *J. Phys. Chem.* **1996**, *100*, 10523.
(66) Shirota, H.; Horie, K. *J. Phys. Chem. B* **1999**, *103*, 1437.
(67) Chakraborty, A.; Seth, D.; Setua, P.; Sarkar, N. *J. Phys. Chem. B* **2006**, *110*, 5359.
(68) Shirota, H.; Segawa, H. *Langmuir* **2004**, *20*, 329.
(69) Fee, R. S.; Maroncelli, M. *Chem. Phys.* **1994**, *183*, 235.